HELIUM PASSIVATION: CALIBRATION WITH IN-ORBIT DATA

B: Zitouni [(1)], I. Fischer[(1)], M. Peukert [(1)]

[(1)] OHB System AG, Universitätsallee 27-29, 28359 Bremen, Email: bayrem.zitouni@*ohb.de*

Abstract

OHB launched its first geostationary satellite in January 2017 and performed the first in-orbit pressurant passivation. The gas was passivated through a venting device located at the bottom of the spacecraft after its arrival in the operational orbit. The passivation is a technical challenge where the passivation time, the physical behaviour of the component and the spacecraft are impacted.

Passivation modelling is performed by coupling the analysis of the propulsion subsystem with a 1D flow simulation and the impact on the spacecraft with a plume impingement analysis.

The paper will discuss the technical challenges related to the passivation by correlating the 1D flow simulation to the behavior observed in orbit. Time of passivation, the remaining mass and pressure is studied. It's shown that the 1D code is suitable to a certain level to reproduce the flow conditions and pressure decay.

Although the venting device is designed as non-propulsive, the expelled gas impinge the spacecraft surfaces. Thus, undesirable effects such as unwanted forces and torques need to be compensated by the Attitude Control System. The plume impingement was correlated by modelling the non-propulsive vent with a CFD tool, extrapolating the outcome in the far field and comparing the results to telemetry data. Results showed that a dynamic accommodation coefficient is not necessary to correctly predict forces and torques.

The presented work is used as guideline to accommodate passivation devices in future OHB satellites. Main lessons learnt regarding passivation analysis will be presented in this paper.

1 Introduction

As presented in [1], recent space passivation requirements implement stringent guidelines for large system integrators to avoid satellite fragmentations due to possible collisions. One of them is to passivate the propulsion subsystem. The strategy of this manoeuver is up to the satellite manufacturer to imagine. Technical challenges are mainly related to the duration of the passivation, the general behaviour of various internal components and the interactions with the spacecraft.

It has to be distinguished between passivation of remaining pressurant in the high-pressure tanks of a chemical bi-propellant propulsion system and passivation of residual propellant. The helium passivation could occur at beginning of life after transfer to operational orbit or after disposal of the spacecraft into graveyard (end of life option). Since the passivation branch is usually isolated by a normally-closed pyro valve, the pressurant passivation is typically performed at begin of life due to lifetime restrictions of the pyro.

This paper presents the implementation of the helium passivation process as performed on-board OHB's first geostationary satellite.

Main lessons learnt were used to better correlate the fluid 1D modelling and plume analysis due to cold gas impinging the spacecraft surroundings.

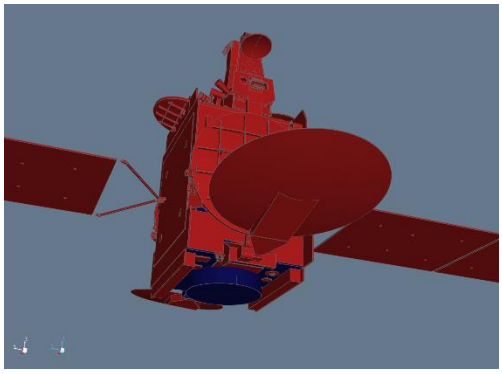

Figure 1: OHB geostationary spacecraft

2 Context: OHB Geostationary spacecraft Passivation

OHB's first geostationary spacecraft was launched January 28, 2017 01:03:34 UTC by a SOYUZ launcher (Soyuz Flight VS16) into standard Geostationary Transfer Orbit (GTO). After successful GTO-to-GEO transfer, the propellant tanks of the chemical propulsion system (CPPS) were isolated from the pressure control assembly (PCA) by means of normally-open pyro valves.

The Chemical Propulsion Subsystem (CPPS) is a pressure-regulated bipropellant propulsion system using MMH (Mono-methyl hydrazine) as fuel and MON-3 (Mixed Oxides of Nitrogen) as oxidizer with GHe as pressurising agent. Correlation of the chemical propulsion subsystem analysis is presented in [2].

Figure 2 illustrates the helium passivation assembly allowing the evacuation of remaining helium from the high-pressure tanks to space through an evacuation valve (EVV) and a non-propulsive vent (NPV). The gas pressure regulator (GPR) reduces the helium pressure to regulated pressure. Downstream of the GPR, a passivation pyro valve is isolating the evacuation valve and the NPV until start of passivation. The pressure evolution during passivation is monitored by a high-pressure transducer (HPT) located next to the tanks and a low-pressure transducer downstream of the GPR.

The high pressure tanks are thermally controlled by two heater lines and dedicated thermistors mounted on the tank shell. In fact, the passivation of the gas will impact the thermal behavior of the tanks.

The monostable Evacuation Valve (EVV) is controlling the passivation in pulse-mode via telecommands.

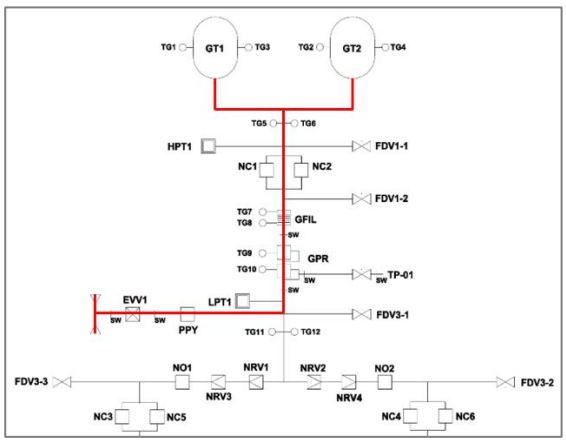

Figure 2: Helium passivation assembly

The non-propulsive vent is equipped with an orifice at each side of the T-shaped fitting. The two orifices serve as flow restrictor and adjust the helium mass flow in accordance with upstream pressure.

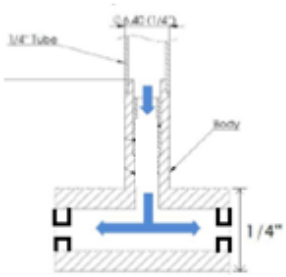

Figure 3: Simplified NPV, narrow exit schematics

The passivation occurred shortly after arrival into geostationary orbit after deployment of the solar arrays and the antennas. The passivation lasted several hours.

	Passivation sequence
Phase 1	Transfer from GTO to GEO
Phase 2	Deployment of solar arrays
Phase 3	Deployment of antennas
Phase 4	Opening of EVV
Phase 5	End of passivation sequence

Table 1: Passivation sequence

During helium passivation, some torque has been observed due to the gas flow impinging on the spacecraft surroundings. These torques were controlled with AOCS system through reaction wheels.

The passivation sequence and the plume impingement have been studied separately as presented in the next sections.

3 Passivation process modelling and calibration with in-orbit data

3.1 Passivation modelling

The passivation was modelled with a 1D fluid software called EcosimPro and its library ESPSS [3]. The first analysis performed during the design phase was updated and correlated with the in-orbit behaviour.

The numerical tool is able to model the whole spacecraft propulsion subsystem by combining different libraries (Fluid 1D, control, thermal etc …).

Standard components like tanks, valves, filters, pipes are contained in the European library called “ESPSS”. Gases and fluid thermo-physical properties are included and extracted from NIST code.

The 1D fluid approach is sufficient to model the passivation process as we are mainly interested in the passivation duration as well as mass flow and pressure evolution. Figure 4 illustrates the EcosimPro model for helium passivation. It consists of two helium tanks, one pressure regulator, one EVV, the non-propulsive vent and tubing.

Helium tanks are modelled as cavities with their Thermal Control System (TCS), exchanging heat with the spacecraft thermal environment and communicating with the rest of the assembly through the pipes. Heaters are activated when the temperature reaches a lower threshold and are turned off when the temperature reaches the upper threshold.

The thermal capacity of the tanks is modelled by taking into account the thermal parameters of its materials. Connection to the spacecraft environment is performed through linear conductors and radiative components.

In the numerical tool, pipes are modelled as 1D nodes where each segment has the correct geometrical properties like length, number of bends, bend radius etc… Special care was given to model the downstream piping system.

The pressure regulator is a standard component in EcosimPro where opening and closing pressure are defined. These parameters were then set according to the telemetry observations.

EVV was modelled as a valve and its pressure drop values calibrated with on-ground testing.

Finally, the NPV assembly took into account a t-fitting and 2 adjacent orifices modelled as junctions. The orifices diameter is derived from the effective area that is depending on a discharge coefficient and the geometric orifice throat area.

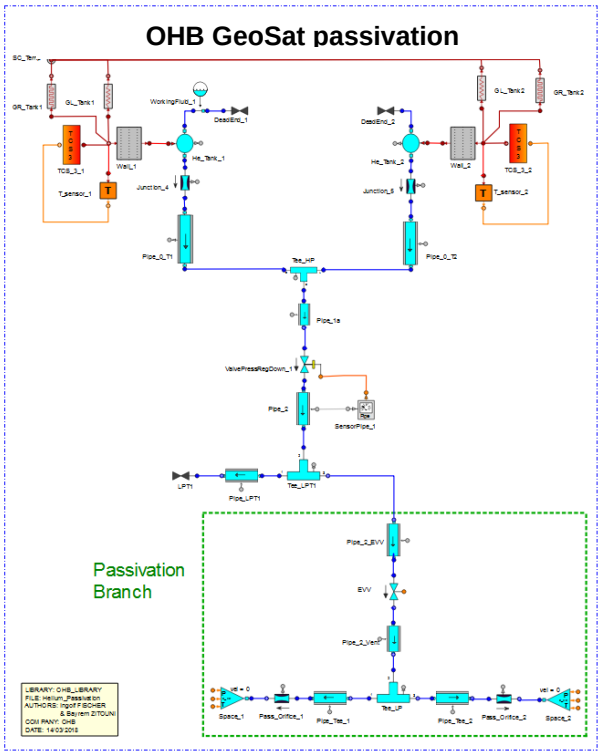

Figure 4: 1D flow modelling of the passivation assembly within the propulsion subsystem

3.2 Passivation calibration with in-orbit data

The passivation calibration was performed by correlating the pressure evolution within the tanks. Therefore, the duration of the process and the mass flow could be deduced, the requirement being that the pressure must decrease until reaching a certain threshold.

In addition to the process duration, correlating the mass flow is very important to calibrate the plume effects. This correlation was performed to tackle the uncertainties due to the manufacturing tolerances. The effective area of the flow restrictor depends on the geometrical area and the discharge coefficient. In this approach, the discharge coefficient was then calibrated to fit the expected and observed mass flow, which compensates the manufacturing uncertainties.

The first step was to extract all EVV pulses from operations sequence during LEOP. The pressure of the tanks and the pressure regulator behaviour in orbit were measured by pressure transducers (shown in the previous section).

The results of the calibration with the right discharge coefficient are in excellent agreement with flight data. The pressure calculated by the 1D flow fits perfectly the data observed in-orbit and matches the pressure within the tanks and the pressure regulators.

It has to be noticed that the passivation duration was observed to be in line with the prediction from the design phases. The average mass flow was in the expected range.

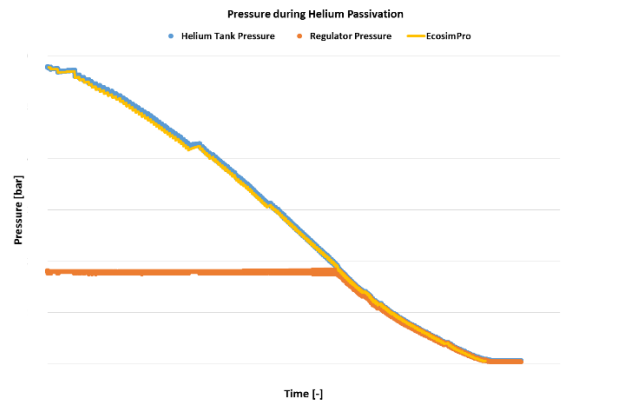

Figure 5: Pressure evolution during Helium passivation

When plotting the differences between simulation and orbit data, the maximum absolute deviation can be deduced to be less than 2%.

However, as the relative uncertainties of the measurement grows when the pressure decreases at the end of the passivation process, the relative error increases. When the average absolute error is investigated, the measured error is in the range of the sensors uncertainties.

	value
Maximum relative error	1.82%
Average relative error	1.15%
Maximum absolute difference	< 900 mbar
Average absolute difference	< 500 mbar

Table 2: Error evolution

The accuracy of the performance predictions were correlated with the regulated pressure uncertainties and the orifice size tolerance due to manufacturing.

The "± x mbar" uncertainties were applied to the in-orbit data and gave an envelope encompassing the simulation data that always remain inside this envelop.

This gives confidence about the 1D fluid simulation approach that in both cases, related to the pressure regulator uncertainties, the simulation still correctly predicts the general behaviour.

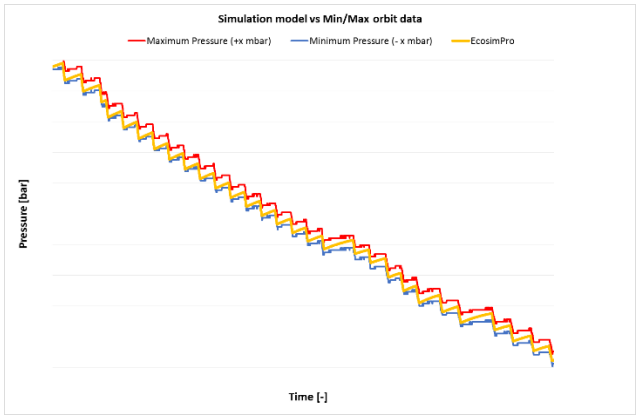

Figure 6: Simulated Pressure compared to the orbit data ± GPR uncertainties

The simulation is however more sensitive to the orifice size and showed that the diameter plays a non-negligible role in the shape of the pressure decrease. It has also to be noticed that due to the 1D approach limitations, no thermal correlation is presented. In fact, in order to correctly correlate the temperature drop during the passivation, a more detailed 2D or 3D model is needed where thermal gradient of the tank can be modelled.

4 Passivation induced plume modelling and calibration with in-orbit data

The gas passivation will also act as a cold gas thruster by impinging the spacecraft surfaces, thus, undesirable effects such as unwanted forces and torques need to be compensated by the Attitude Orbit Control System.

4.1 Cold gas plume modelling

As stated in [1] and in [3], OHB developed a CFD method coupled to ray-tracing approach to model the cold gas plume impingement. openPlumeCGT (Cold Gas Thruster) was developed around openFoam for the CFD part, python scripts for extrapolation in the far field and paraview or Systema to plot the results.

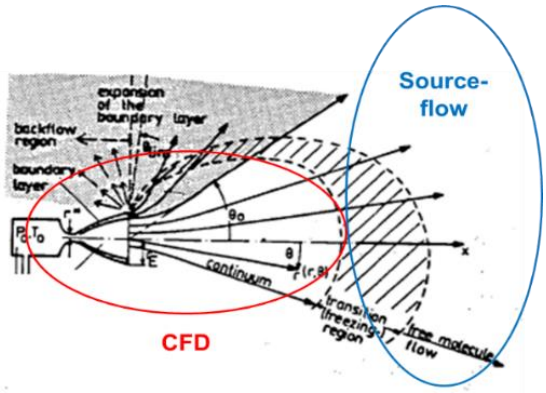

Figure 7: CFD + source flow method

The method was first developed because the existing commercial CFD software was not able to model non conic shapes. Then, in the frame of another project, a trade-off has been made between different venting devices.

openFoam models the Navier-Stokes equations: the equation for conservation of mass (also called continuity) is given in Equation 1. Conservation of momentum is described by Equation 2. Finally, Equation 3 is the equation for energy conservation.

$$\frac{\partial \rho}{\partial t} + \boldsymbol{\nabla} \cdot [\boldsymbol{u}\rho] = 0 \qquad \textit{Equation 1}$$

$$\frac{\partial (\rho \boldsymbol{u})}{\partial t} + \boldsymbol{\nabla} \cdot [\boldsymbol{u}(\rho \boldsymbol{u})] + \nabla p - \boldsymbol{\nabla} \cdot \boldsymbol{T} + \boldsymbol{f} = \boldsymbol{0} \qquad \textit{Equation 2}$$

$$\frac{\partial (\rho E)}{\partial t} + \boldsymbol{\nabla} \cdot [\boldsymbol{u}(\rho E)] + \boldsymbol{\nabla} \cdot [\boldsymbol{u} p] + \boldsymbol{\nabla} \cdot (\boldsymbol{T} \cdot \boldsymbol{u}) + \boldsymbol{\nabla} \cdot \boldsymbol{j} = 0 \qquad \textit{Equation 3}$$

In these equations, ρ is the density of the fluid, $\boldsymbol{u}$ is the fluid velocity, t represents time, p is the pressure, $\boldsymbol{T}$ is the viscous stress tensor, $\boldsymbol{f}$ is the sum of the body forces working on the fluid, E is the total energy of the fluid and $\boldsymbol{j}$ represents diffusive heat flux.

openPlumeCGT has been validated numerically by comparison to another CFD tool and physically with regard to available on-ground experiments performed in DLR [5] with Nitrogen.

In the case of the OHB geostationary satellite, the passivation device, in form of a narrow exit, have been modelled with two approaches: a conic model and an orifice model. Both of the devices were modelled in the course of [1] and the density, pressure and velocity fields were obtained with openFoam 2.3.

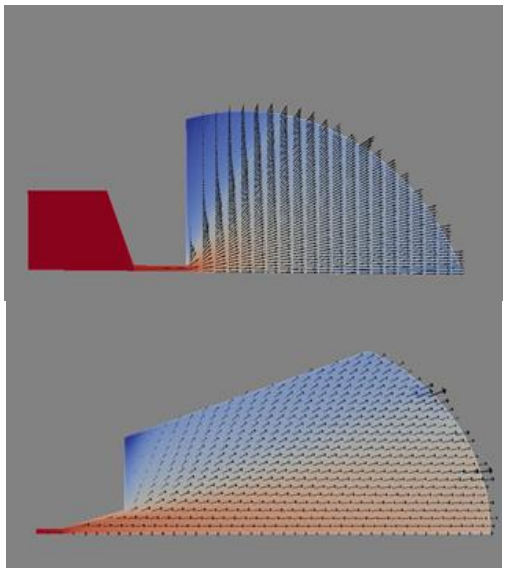

Figure 8: Gas densities for NPV Narrow exit (up) and conic exit (down)

The goal of the calibration in orbit was to correlate the gas plume and get more confidence in the CFD part. In fact, it was observed that the conic exit model focused the plume in the center compared to the narrow exit as seen in Figure 9.

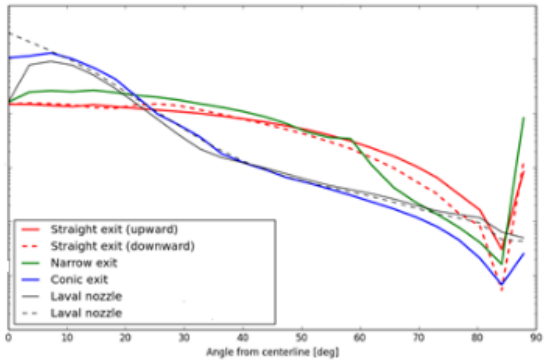

Figure 9: NPV densities variation with angles from centerline

The density, pressure and temperature are interpolated at the starting points and extended according to isentropic expansion laws (Equation 4).

In this equation, r indicates the distance from the centre of the nozzle exit, V is the volume available to the fluid, while ρ, p and T are the common flow variables density, pressure and temperature. The subscript 1 indicates the starting point of a streamline, while the subscript far indicates a point on the streamline which is farther away.

$$\rho_{far} = \rho_1 \frac{V_1}{V_{far}} = \rho_1 \frac{r_1^2}{r_{far}^2}$$

$$p_{far} = p_1 \left(\frac{r_1^2}{r_{far}^2} \right)^{\gamma} \qquad \text{Equation 4}$$

$$T_{far} = T_1 \left(\frac{r_1^2}{r_{far}^2} \right)^{\gamma - 1}$$

Figure 10 illustrates the process: the red box shows the selected starting points. These all lie within the CFD domain that results from OpenFOAM, indicated by the blue points. After interpolation to obtain the values of density, temperature and pressure on the red points, Equation 4 is used to find the values in the green points, forming the far field. The far field extends to a user-defined distance.

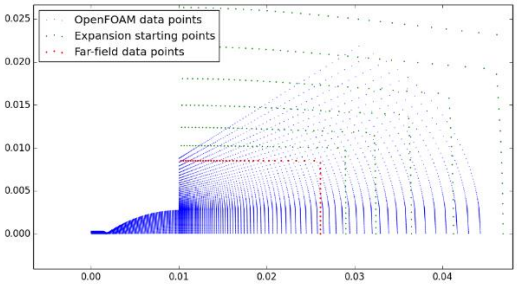

Figure 10: Example of far-field calculation

4.2 Plume correlation with in-orbit

The passivation device is located in the bottom of the spacecraft, indicated by the yellow circle.

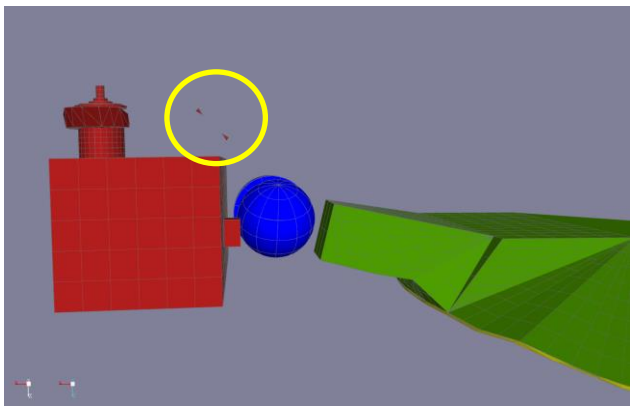

Figure 11: Passivation device location

The results were compared to the observed in-orbit torques.

As the passivation was performed in pulse mode. The measured torque generated varies and is not constant due to measurement uncertainties from AOCS system. When plotted, the torque average is however constant during the process and decreases at the end of the passivation as the quantity of Helium inside the tanks becomes smaller.

Compared to the in-orbit generated torque, the conic exit model is overestimating by 20% whereas the narrow exit is overestimating by 10%.

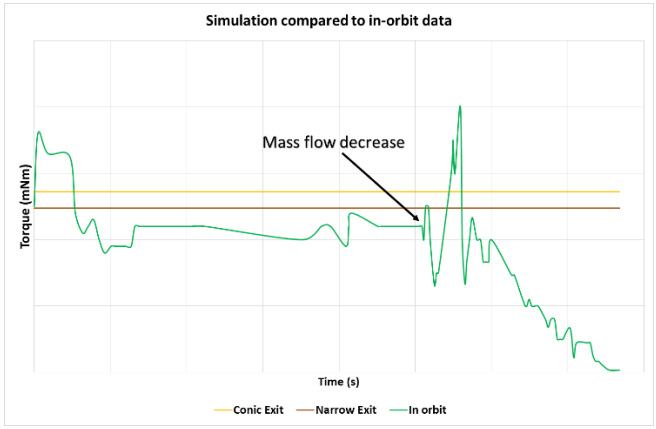

Figure 12: Plume calibration with in-orbit

This is due to the fact that the plume is more centered in the case of the conic modelling. Spreading the plume leads to less torque as the flow is not focused on the impinged object.

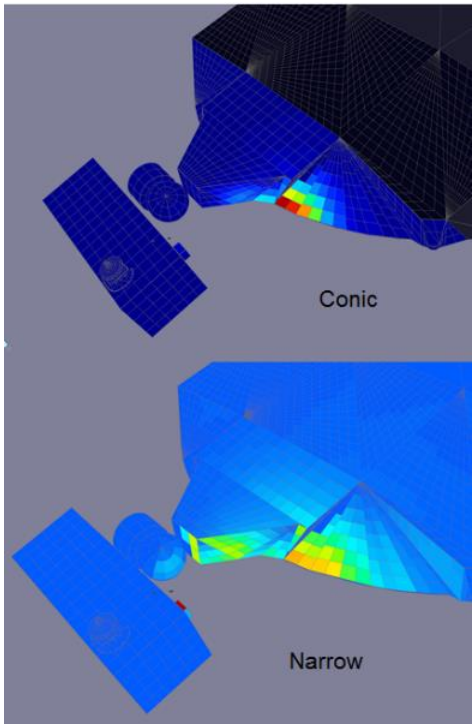

Figure 13: Gas densities for NPV Narrow exit (up) and conic exit (down)

The plume characteristics around the impingement can be extracted from the simulation. Located at several centimeters, the flow is rather in a transition phase according to its Knudsen number. The impinging angles w.r.t “thruster” axis angle vary from 10° to 20°.

It has to be noticed that the method was validated compared to an on-ground testing of another gas. In the specified region, the difference is about ±15% when the correct nozzle is modelled.

Angle	Simulation deviation w.r.t experiment
0	35%
10	**13%**
20	**-17%**
30	29%
40	38%
50	28%
60	25%
70	-4%

Table 3 Simulation deviation with regard to the experiment

During the validation campaign, several domains were tested as shown in Figure 14. After the calibration with the on-ground testing, a guideline was extracted to choose the right starting domain. The physical properties of the flow, such as the Reynold number, were linked to the dimension of the domain (height and length).

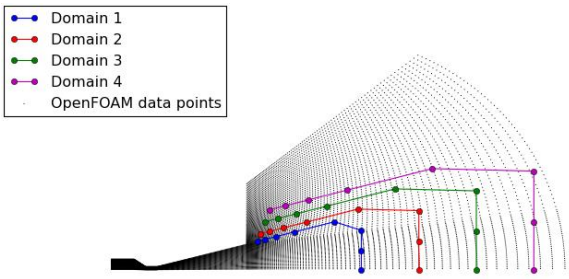

Figure 14: Different starting domains for extension method

These guidelines were thus applied in the final correlation of OHB geostationary satellite. The in-orbit data showed that this approach can be trusted since the overestimation of the observed torque is in the same range as the validation showed (±15% vs 10 to 20%).

In addition, due to the low differences with regard to in-orbit data, no further investigation were carried out to correlate the plume results with the dynamic accommodation factor that depends on the impinged material. In fact, the main driver for the cold gas impingement modelling is the chosen CFD approach and the starting domain for interpolation.

5 Conclusion

The calibration in-orbit gave OHB important information about the modelling capabilities within the propulsion department. The fluid 1D results were in excellent agreement with in-flight data. The pressure decrease was perfectly reproduced with less than 2% precision when compared to in-orbit data. However, the correlation also showed the limitation of a 1D approach when trying to fit temperature data of larger components such as tanks.

The plume analysis showed that the CFD approach coupled to a far field extrapolation can be trusted. The good surprise came from the fact that the plume analysis was spot on the in-orbit results. And this was done without any correlation of the dynamic coefficient of the impinged elements. Even if the observed torque was in the range of some milli-Newton meters, the plume method was able to reproduce the final result with an overestimation of only 10%.

For a first in-orbit passivation, results are encouraging and will be used in the next OHB spacecrafts.

6 Acknowledgement

The authors would like to thank their OHB colleagues for their valuable contribution: S. Beekmans and R. Viroli for the operational part, N. Neumann for the AOCS part. The plume impingement part was developed with L. Denies during his internship in OHB.

7 References

[1] B. Zitouni, L. Denies, M. Peukert “Comparison of Methods and Devices for High Pressure Vessel Passivation”, SPC 2016
[2] I. Fischer, S. Beekmans, M. Peukert “Chemical propulsion in-flight experience and analysis correlation”, SPC 2018
[3] EcosimPro/ESPSS: software user manual
[4] B. Zitouni et. al. “Chemical propulsion induced plume: openPlume modelling approach”, SPC 2018
[5] K. Plahn and G. Dettleff (2000): Modelling of N2-thruster plumes based on experiments in STG. AIP Conf. Proc. 585, 848 (2001); 9-14 July 2000, Sydney (Australia).